Physics – Uspekhi **59** (12) 1258 – 1265 (2016)

CONFERENCES AND SYMPOSIA

PACS numbers: 73.20.Mf, **78.55. – m**, 78.67.Hc

125th ANNIVERSARY OF THE BIRTH OF S I VAVILOV

Fundamental and applied aspects of luminescence of colloidal quantum dots

V F Razumov

DOI: https://doi.org/10.3367/UFNe.2016.03.037861

Contents

Abstract. The spectral luminescent characteristics of colloidal quantum dots as a new class of luminophores are discussed and state-of-the-art investigations, problems, and prospects for their applications are considered.

Keywords: colloidal quantum dots, luminescence quantum yield, luminescence lifetimes, luminescence blinking, multiple exciton generation, quantum size effect

1. Introduction

Luminescence as a physical phenomenon has very long been known, and many great scientists that made basic contributions to natural science have attempted to understand its nature for several centuries. In his opening talk at the Second All-Union Conference on Luminescence in 1948, S I Vavilov presented in outline the historical development of the science of luminescence and named a number of outstanding scientists that had made important contributions to the understanding of this phenomenon, among them Boyle, Newton, Lomonosov, Euler, Boshkovich, Petrov, Arago, Brewster, Stokes, Becquerel, and Lomel [1]. The study of luminescence, as S I Vavilov pointed out, is a prominent example of the close relationship between fundamental and applied investigations. On the one hand, luminescence plays an important role for practical applications as a light source, and, on the other hand, studies of luminescence have led to the discovery of new physical phenomena such as radioactivity, while the luminescent technique itself has become an efficient tool for studying the structure and properties of matter.

The work by S I Vavilov and his scientific school played an outstanding role in the development of luminescence science. In this work, the scientific definition of luminescence was proposed and basic laws governing the transformation of different types of energy to light energy in luminophores were formulated: the Vavilov law of the independence of luminescence spectra on the exciting light wavelength, the Levshin mirror symmetry rule, and Stepanov's relation between absorption and emission spectra of luminophores.

There are two types of luminophores — organic and inorganic. Organic luminophores include organic or organoelemental molecules having a high photoluminescence quantum yield. They are exploited for luminescent assay and diagnostics in physics, chemistry, biology, medicine, and criminalistics, as well as in the production of various luminescent materials and fluorescent dyes. The glowing of inorganic luminophores is caused, as a rule, by luminescent ions, for example, cations of transition and rare-earth elements contained in small amounts in crystals absorbing light. Inorganic luminophores are employed in luminescent lamps and cathode ray tubes, for manufacturing X-ray displays, as radiation sensors, etc. The spectral luminescent properties of organic luminophores required for various purposes are achieved by the proper chemical design of the structure of luminescent molecules. For inorganic luminophores, this is achieved by the appropriate choice of the chemical composition of luminescent activators.

Currently, more and more attention, from both the fundamental and practical points of view, is being devoted to a new class of luminophores, so-called colloidal quantum dots (CQDs) with luminescent properties determined by the

V F Razumov Institute of Problems of Chemical Physics, Russian Academy of Sciences, prosp. Akademika Semenova 1, 142432 Chernogolovka, Moscow region, Russian Federation
E-mail: razumov@icp.ac.ru

Received 25 May 2016, revised 6 July 2016
Uspekhi Fizicheskikh Nauk **186** (12) 1368 – 1376 (2016)
DOI: https://doi.org/10.3367/UFNr.2016.03.037861
Translated by M N Sapozhnikov; edited by A Radzig

average size of nanoparticles of a crystalline semiconductor, varying within the range of 2–10 nm. In this case, the width of the luminescence spectrum of a single nanoparticle at room temperature is only 20–30 nm, while the spectrum position can be varied within about 100 nm with respect to the bandgap width of a bulk semiconductor. Thus, a rather limited set of luminescent variable-size quantum dots based on $A^{II}B^{VI}$, $A^{III}B^{V}$, or $A^{IV}B^{VI}$ semiconductors easily covers the spectral range from 350 to 3500 nm.

The dependence of the spectral luminescent properties of ultradispersion semiconductors on particle size was demonstrated for the first time in 1981 by Ekimov and Onushchenko [2] at the Vavilov State Optical Institute for CuCl nanoparticles grown in multicomponent silicate glasses during thermally induced diffusive phase decomposition of a supersaturated solid solution. This dependence was theoretically justified by Efroses [3]. Independently, Brus [4, 5] obtained the same dependence for colloidal CdS solutions. Over the next several years this effect was experimentally revealed and confirmed for ultradispersion particles of CdS, CuBr, CdSe, PbS, ZnS, Zn_3P_2, and Cd_3P_2 semiconductors [6–11]. The term 'quantum dot' appeared for the first time in 1988 [12] and since then has been used in the literature instead of the terms 'ultradispersion particles' or 'nanocrystals'.

In the early 1990s, a precision physical method for producing quantum dots by molecular beam epitaxy was developed [13]. The method is based on the deposition of a thin layer of a semiconductor material onto an atomically smooth substrate, which spontaneously decomposes after achieving a critical thickness of a few monomolecular layers, producing a regular structure of quantum dots in the form of rectangular small pyramids [14]. This method is quite complicated and requires precision and costly equipment, but provides a very narrow size distribution of epitaxial quantum dots. At present, they are finding wide applications in various optoelectronic devices. Notice, however, that epitaxial quantum dots fundamentally differ from colloidal quantum dots in their properties and applications. At the same time, they represent a new class of luminescent nanostructures in classical quantum electronics based on the quantum size effect.

In 1993, a simple and very efficient chemical method for synthesizing quantum dots was proposed [15], which was called high-temperature colloidal synthesis (HTCS). The method uses high-boiling trioctyl phosphine oxide (TOPO), which is simultaneously a solvent, cationic complexing agent, and anticoagulant forming the ligand shell of CQDs. In this case, a trioctyl phosphine (TOP) molecule, which is structurally isomorphic to TOPO, plays the role of a nonmetal complex agent and is also involved in the formation of the ligand CQD shell. This method not only opened up new possibilities for CQD studies but also demonstrated real prospects for their practical applications. The further development of HTCS is directed to the search for new high-temperature solvents efficiently stabilizing the CQD surface and to the development of methods for post-synthetic CQD modification to obtain high luminescence quantum yields [16]. Unlike organic molecular luminophores, CQDs have, in principle, much higher thermal stability and photostability and, in addition, offer a number of functional advantages due to the unique possibility of varying their spectral parameters. Already at present, they are finding applications in LEDs, displays, solar cells, optical amplifiers, lasers, chemical and biological sensors, and biomedical diagnostics. Further promising applications of CQDs concern molecular electronics and quantum computers.

The importance of this scientific field and the priority of the pioneering work that initiated the development of this new field of photonics, which is being extensively developed at present, was recognized by awarding the Robert Wood Prize in 2006 to Louis Brus, Aleksei Efimov, and Alexander Efros. In 2008, Louis Brus was awarded the Fred Cavli Prize in the nanotechnology category. The relevance of this field is also confirmed by the fact that for the last five years more than 10,000 papers in this field have been published in scientific journals indexed in the Scopus and Web of Science databases. At a recent international conference in Paris devoted to the 30th anniversary of the discovery of quantum dots, new ideas were proposed and prospects for QD applications were outlined (www.30-years-qds.com).

In this paper, based on the oral report presented at the 40th Vavilov Readings devoted to the 125th anniversary of S I Vavilov's birth, the main focus is devoted to the spectral luminescent properties of CQDs and new physical effects determining their unique characteristics, opening up new possibilities for their application.

2. Quantum size effect

Size effects in semiconductors have a quantum nature and are related to the appearance of energy quantization conditions caused by spatial restriction on the motion of quasiparticles. This attracted attention back in the 1930s, at the dawn of quantum mechanics. For example, studies of the electric breakdown in dielectrics revealed anomalous critical values of the electric breakdown potential for gaps lower than 10^{-6} cm, which were inconsistent with classical concepts [17, 18]. In the 1960s, a number of quantum size effects were discovered in the conductivity of thin semiconductor and semimetal films [19]. The quantum size effect in the absorption of light in semiconductors was experimentally demonstrated for the first time in paper [20] for so-called quantum wells consisting of a thin epitaxial narrow-gap semiconductor film located between two wide-gap semiconductor layers. When the motion of charge carriers in a semiconductor is spatially restricted in one of the three directions, quantization conditions for admissible energy values appear, according to which an integer number of de Broglie half-waves should fit in a given spatial size. As a result, various quantum size effects appear in spatially restricted semiconductors, which are caused by a radical change in the density of electron states in the semiconductor. Quantum size structures can be classified by the dimensionality of the free motion of electrons and holes. These are two-dimensional (2D) structures (quantum wells), one-dimensional (1D) structures (quantum wires), and zero-dimension (0D) structures (quantum dots).

The type of electron structure of a quantum dot and its dependence on the nanoparticle size are determined by the solution of the stationary Schrödinger equation in a spherically symmetric rectangular potential well [21]. The solution to this problem gives the theoretical foundation for determining the size dependence of transition energies during the absorption and emission of light by a quantum dot. When the nanoparticle size becomes small enough, the continuous spectrum of allowed energies for electrons and holes in a semiconductor transforms into a discrete spectrum (Fig. 1).

The corresponding stationary energy levels $E_{n_e l_e}$ and $E_{n_h l_h}$ of electrons and holes, respectively, are described by the

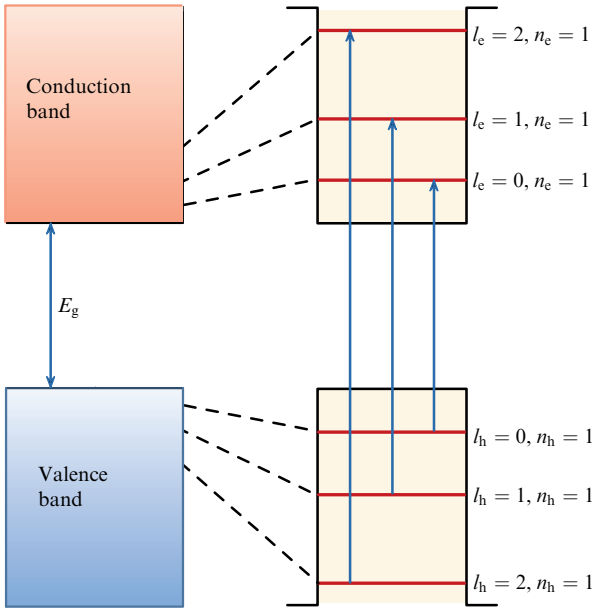

Figure 1. Schematic of the transformation of the energy spectrum of charge carriers in a semiconductor particle upon decreasing its size from macroscopic to a few nanometers.

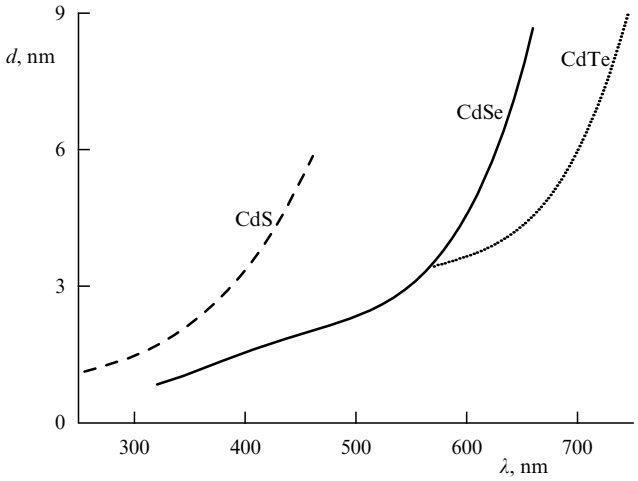

Figure 2. Dependences of the diameter of colloidal quantum dots on the position of the longest-wavelength absorption band of CdTe, CdSe, and CdS (taken from Ref. [22]).

expressions

$$E_{n_e l_e} = \frac{\hbar^2 \rho_{n_e l_e}^2}{2 m_e R^2}, \quad E_{n_h l_h} = \frac{\hbar^2 \rho_{n_h l_h}^2}{2 m_h R^2}, \tag{1}$$

where R is the quantum well radius, m_e and m_h are the effective electron and hole masses, respectively, n_e, l_e, n_h, and l_h are the principal and orbital quantum numbers of the corresponding electron and hole states, and $\rho_{n_e l_e}$ and $\rho_{n_h l_h}$ are a set of numbers determined by the roots of spherical Bessel functions. The first three nonzero roots in the increasing order $\rho_{10} = 3.142$, $\rho_{11} = 4.493$, and $\rho_{12} = 5.763$ correspond to quantum states 1S ($n = 1, l = 0$), 1P ($n = 1, l = 1$), and 1D ($n = 1, l = 2$). The selection-rule allowed transitions between the ground state of a particle and its excited states with quantum numbers n_e, l_e, n_h, l_h determine the absorption and emission spectra of quantum dots (see Fig. 1). Expressions (1), taking into account the Coulomb interaction of electrons and holes, give the Brus formula [11] allowing the estimate of the value of ΔE determining the shift of the absorption and luminescence spectra of nanoparticles as a function of their size:

$$\Delta E \approx E_{10}^{e} + E_{10}^{h} - E_g = \frac{\hbar^2 \pi^2 (m_e + m_h)}{2 R^2 m_e m_h} - \frac{1.8 e^2}{\varepsilon R}. \tag{2}$$

Here, E_g is the bandgap width of a bulky semiconductor, R is the nanoparticle radius, and ε is the permittivity. The second term on the right-hand side takes into account the Coulomb interaction of an electron–hole pair in CQDs. This expression is often used to estimate the mean size of CQDs. However, in reality the size dependence of the position of the long-wavelength absorption edge does not strictly follow the Brus formula. Because of this, the size of particles is determined in practice from experimental spectral dependences such as those presented for cadmium chalcogenide in Fig. 2.

To obtain such calibration dependences, it is necessary to record absorption spectra for a series of samples with particles and to measure particle sizes through the method of electron microscopy or X-ray diffraction by the broadening of observed peaks. The measurement of extinction coefficients of CQDs is more complicated. It was reliably found that the extinction coefficient in the short-wavelength region of the absorption spectrum is proportional to the volume of particles [23]. However, data on the size dependence of the extinction coefficient in the region of the long-wavelength absorption maximum are contradictory. Thus, according to theory [5], the extinction coefficient in this region should be almost independent of the particle size. This was confirmed in experiments for CdTe [24]. However, for CdSe [25, 26] and PbS and PbSe [23], linear dependences of the extinction coefficient on the particle diameter were observed. The dependence with the exponent 1.6 was observed in Ref. [27] for CdS. At the same time, in Ref. [22] approximately cubic size dependences were observed for CdTe, CdSe, and CdS, which is wholly inconsistent with theory [5].

The phonon spectrum of CQDs also somewhat changes due to spatial restrictions. This is manifested in the change to characteristic Raman frequencies [28–32].

3. Luminescence blinking effect

Due to various reasons which we will consider below, even CQDs with very close sizes can have very different spectral luminescent properties. This is related to the defect structure of the surface of nanoparticles and the presence of local states of different types in which photoelectrons or photoholes can be trapped. As a result, a CQD becomes charged and the luminescence quantum yield of such a nanoparticle sharply decreases, manifested in the so-called fluorescence blinking effect observed for single nanoparticles, which can be during observation in one of the two states: luminescent (ON) and nonluminescent (OFF). Transitions between these states occur randomly on a broad time scale, from 10^{-6} to 10^{1} s. The luminescence blinking effect depends on the CQD synthesis conditions, the composition, structure, and form of the ligand shell, the thickness of the additional semiconductor shell, and many other factors. The blinking effect was observed for the first time by Nirmal et al. [33]. As a rule, it is studied by the spectroscopy of single nanoparticles [34, 35]. The state-of-the-art in these investigations is presented in a

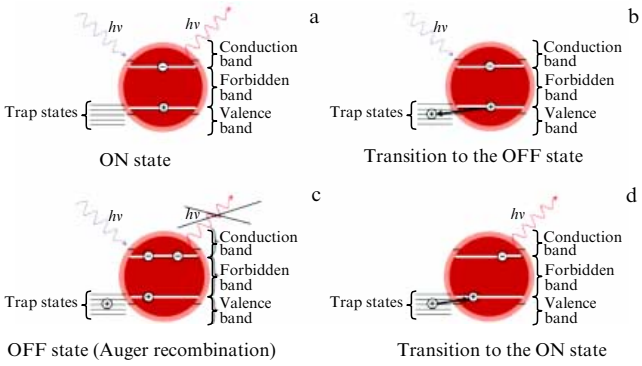

Figure 3. Luminescence blinking mechanism. (a) The ON state: photon absorption is followed by emission. (b) Transition to the OFF state: photon absorption is followed by hole capturing in a trap. (c) Radiationless deactivation of the OFF state after photon absorption due to Auger recombination. (d) The radiative ON state is recovered after the spontaneous transition of a hole from a trap to the valence band.

number of recent reviews [34, 36–39]. One of the first mechanisms proposed for explaining the CQD blinking effect assumes the transition of a nanoparticle absorbing a photon to the charged state (the OFF state) in which the radiationless Auger recombination occurs after each subsequent absorption of a photon [40] (Fig. 3). The reverse transition to the ON state occurs due to spontaneous CQD discharge [41] (see Fig. 3).

This mechanism was modified in following papers mainly to refine the charge state type and its production and discharge [42–45]. Essentially different mechanisms were also proposed [35, 46, 47]; however, complete clarity is lacking to date. This is explained by the complexity of the process itself and difficulties in obtaining experimental data and their interpretation. It is only clear that the surface states of nanoparticles play an important role. The state-of-the-art in studies of the mechanism of CQD luminescence blinking is presented in review [48]. The blinking effect reduces the fluorescence quantum yield of an ensemble of CQDs as a whole [34]. In this case, as shown in Refs [49, 50], the luminescence quantum yield of some single CQDs in the ensemble is close to unity, whereas other CQDs do not luminesce at all. In addition, some intermediate state is possible in which excited CQDs emit photons, but with a lower probability than in the ON state [51].

The suppression of the blinking effect has been widely studied. One of the efficient methods for suppressing blinking is based on growing additional wider-gap semiconductor shells on CQD cores. The accumulation of additional semiconductor shells requires maximum matching between the lattice parameters of the core and shell materials and the controllable shell thickness to avoid the appearance of defects at the interface between two semiconductors. The authors of paper [52] reported a new class of CQDs with shells containing up to 19 monolayers of the accumulated semiconductor. The fraction of blinking particles in such CQDs is reduced to 20%, whereas usually it is difficult to make it lower than 70%. It was shown in Ref. [53] for InP@CdS CQDs that the blinking effect and Auger recombination were suppressed upon increasing the CdS shell thickness from 1 to 11 monolayers. In addition, the photostability of single CQDs and the CQD ensemble as a whole considerably increases. The suppression of luminescence blinking with an increase in the shell thickness was also observed in Ref. [54]. In paper [55], a luminescence quantum yield as high as 0.94 was reported for CdSe@CdS CQDs with a comparatively small 2.4-nm thickness of a shell consisting of seven monolayers. In Ref. [56], it was shown that the distribution of the lifetimes of the ON and OFF states in $CdSe/Cd_xZn_{1-x}S$ CQDs strongly depended on the zinc concentration in a shell changed in the radial direction. The authors of Ref. [57] showed that the best blinking suppression was achieved for CQDs with the complex CdSe/CdS/ZnS shell, where the longest ON states were observed.

Among other factors suppressing luminescence blinking, the ligand environment plays an important role. The efficient suppression of luminescence blinking by thiol ligands was demonstrated for water-soluble CdTe CQDs [58]. The authors of Ref. [58] explain blinking suppression by the removal of surface traps due to the efficient coordination of thiol ligands with vacant cadmium atoms and the formation of the CdS layer. The authors of Ref. [57] reported that in a number of cases thiols, on the contrary, enhanced blinking. The enhancement of blinking was also observed for Mn-doped ZnSe CQDs. CQD fluorescence blinking also depends on other factors, such as the synthesis condition and UV radiation [59], the nearest environment [60], and the pH of the medium [61]. Blinking can be suppressed near the surface of a silver film [62] or an indium-tin oxide (ITO) film [63], and near silver [64] or TiO_2 [65] nanoparticles.

4. Multiple exciton generation

Colloidal quantum dots absorbing photons with an energy several times higher than ΔE determined by the Brus formula (2) reveal a unique effect, which was called in the literature as multiple exciton generation (MEG). In this case instead of the usual radiationless relaxation of electronic excitation, CQDs can generate additional excitons whose maximum number is determined by the ratio of the exciting photon energy to ΔE. For example, the authors of Ref. [66] reported the generation of seven excitons in a PbSe CQD absorbing a photon with an energy 7.8 times higher than the bandgap energy. This corresponds to the conversion of only 10% of the photon energy to heat.

MEG was experimentally observed for the first time in PbSe CQDs [67]. Later, MEG was discovered in CQDs with different compositions, such as PbS, PbTe [68], PbS_xSe_{1-x} [69], CdSe [70], CdTe [71], InAs [72], InP [73], and silicon [74]. A possible MEG mechanism was proposed in 2001 [75], i.e., before its experimental examination. Because the electronic structure of CQDs is a set of discrete energy levels separated by distances greatly exceeding characteristic phonon energies, the usual vibrational relaxation of the electronic excitation can be hindered, because transitions to the next lower electronic level should occur due to simultaneous creation of a great number of phonons. The probability of this process is rather low; therefore, is was assumed that the cooling of hot carriers in CQDs can be considerably slowed down. This phenomenon was called a bottleneck in CQDs. In this situation, the cooling of hot carriers competes with the efficient impact ionization in which a hot exciton generated after high-energy photon absorption transfers its excess energy to one of the valence electrons, creating simultaneously a new exciton (Fig. 4).

However, experimental studies have shown that this mechanism is not always consistent with experimental

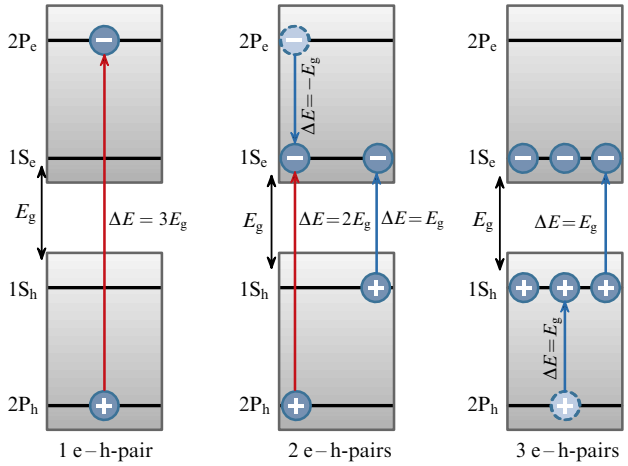

Figure 4. Schematic of the generation of three excitons after the absorption of a photon with an energy more than three times higher than the bandgap width.

results. For example, it was found that the relaxation rate did not decrease with decreasing CQD size despite the increase in the energy level separation [76]. Because of this, some other mechanisms were also proposed for describing MEG [77]. One of them assumes the generation of a biexciton via the virtual single- or biexciton state. This mechanism was considered for the first time in Ref. [78] as an addition to impact ionization. Another MEG model assumes that photon absorption leads to excitation of a superposition of quantum states corresponding to all possible states, including multi-exciton states [79].

MEG is usually observed by the method of pump-probe spectroscopy, allowing measurement of the number of generated excitons. A few attempts to observe MEG in real photovoltaic cells have confirmed that for photon energies exceeding the bandgap width some characteristics improved, but the effect was insignificant for different reasons. For example, an increase in the electron current was observed in a Graetzel cell [80]. However, the energy conversion efficiency was very low because of a weak absorption of light by the CQD monolayer. For photons with energy three times higher than the bandgap width, the authors of Ref. [81] obtained a MEG efficiency equal to 114%, with a total efficiency reaching 4.5%. They assumed that the characteristics of the photovoltaic cell can be improved during optimization.

Thus, for practical MEG applications, it is necessary to solve the intricate problem of the efficient separation of corresponding MEG charges before their recombination, for example, by charge transfer to the electron or hole acceptor attached to the QD surface. However, as pointed out in Ref. [82], the treatment of the QD surface can suppress MEG and, therefore, this should be performed carefully. As far as we know, the complete dissociation of all excitons being produced in MEG was achieved only in Ref. [83] for PbS/methylene blue CQD complexes. The MEG efficiency amounted to 112%.

5. Inhomogeneous broadening of luminescence spectra

Unlike traditional luminophores whose luminescence properties are determined by the electronic structure of single molecules or atoms, CQDs cannot be treated as strictly identical luminescent particles. Their characteristics always have a dispersion caused by the size distribution, which in turn results in the inhomogeneous broadening of the CQD absorption and luminescence spectra. In Ref. [84], a method for separating the homogeneous and inhomogeneous broadenings of CQD luminescence spectra was proposed, which is based on the Kennard–Stepanov–van Roosbroeck–Shockley relation. In 1918, based on Kirchhoff's law and general phenomenological properties of photoluminescence (the independence of the luminescence spectrum of the excitation wavelength, the linear dependence of the luminescence intensity on the exciting light intensity), Kennard [85] concluded that for 'cold' luminescence emission a simple analytic relation between absorption and emission spectra should exist in the form

$$\frac{F(\nu)}{\varepsilon(\nu)} \propto F_{\mathrm{B}}(\nu)\,, \tag{3}$$

where ν is the wave number, $F(\nu)$ is the luminescence spectrum, $\varepsilon(\nu)$ is the absorption spectrum, and $F_{\mathrm{B}}(\nu)$ is the equilibrium blackbody thermal radiation spectrum described by the Planck law. However, Kennard's work was long forgotten and mentioned for the first time only in 1962 [86] after Stepanov [87] considered in 1956 radiative transitions between equilibrium vibrational levels of the ground and excited states in polyatomic molecules and used the relation between Einstein coefficients to obtain an expression similar to formula (3). Stepanov's expression differs only in that the blackbody radiation spectrum was used in the short-wavelength limit:

$$\frac{F(\nu)}{\varepsilon(\nu)} \propto \nu^2 \exp\left(-\frac{hc\nu}{k_{\mathrm{B}}T}\right), \tag{4}$$

where h is the Planck constant, c is the speed of light in a vacuum, k_{B} is the Boltzmann constant, and T is the absolute temperature. Because the photon energy usually greatly exceeds $k_{\mathrm{B}}T$, relations (3) and (4) can be considered equivalent. Also, independently of Kennard's work, the relation between absorption and luminescence spectra was found in 1954 by van Roosbroeck and Shockley applied it to semiconductors [88].

Experimental verification of the Kennard–Stepanov–van Roosbroeck–Shockley relation showed that it is well fulfilled for most dyes [89, 90] and semiconductor layers [91–93]. These relations are also valid for CQDs. Assuming Gaussian shapes of absorption and luminescence bands, relations (3) and (4) give the Stokes shift for a single luminophore particle:

$$\Delta\nu = \frac{hc(\delta\nu)^2}{k_{\mathrm{B}}T}\,, \tag{5}$$

where $\delta\nu$ is the homogeneous width of the luminescence band. Thus, the Stokes shift for traditional luminophores is determined by the homogeneous width of the spectral bands. For an arbitrary CQD ensemble with a certain size distribution characterized by dispersion $\delta\nu_0$ (i.e., the standard deviation of the maximum position from the mean value) due to the quantum size effect, the observed width of the spectral band is given by

$$\delta\nu_{\Sigma} = \sqrt{(\delta\nu)^2 + (\delta\nu)_0^2}\,. \tag{6}$$

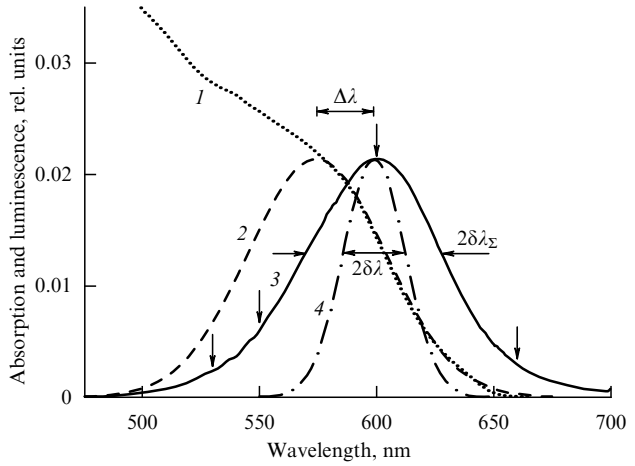

Figure 5. Absorption (curve *1*) and luminescence (curve *3*) spectra of InP@ZnS CQDs. Curve *2* is a Gaussian fitting of the long-wavelength edge of the absorption spectrum. Curve *4* shows the calculated luminescence spectrum for zero inhomogeneous broadening. The horizontal arrows mark the Stokes shift $\Delta\lambda$ and widths of luminescence spectra (doubled standard deviations $2\delta\lambda$ and $2\delta\lambda_\Sigma$). The vertical arrows denote the wavelengths 530, 550, 600, and 660 nm at which luminescence lifetimes were measured.

At the same time, the Stokes shift will also be determined by expression (5), i.e., by the homogeneous width of the luminescence band of individual CQDs. This means that the Kennard–Stepanov relation is not formally valid for the CQD ensemble with a finite dispersion of the size distribution function, but by calculating the homogeneous width from formula (5), we can find the inhomogeneous broadening from formula (6).

Figure 5 shows the absorption and luminescence spectra of InP@ZnS CQDs [94]. The half-width of the luminescence band and the Stokes shift measured in this experiment are 70 nm and $\Delta\lambda = 24.2$ nm, respectively. The homogeneous half-width of the luminescence band found from the Stokes shift by formula (5) is 31 nm, while the inhomogeneous broadening found from formula (6) is 63 nm.

The polydispersity of the given CQD ensemble can be determined from the inhomogeneous broadening by using the experimental calibration size dependence for InP [95] and expression

$$\frac{\delta\lambda_0}{\langle\lambda_0\rangle} = \left(1 - \frac{\langle\lambda_0\rangle}{\lambda_{\max}}\right)\frac{\delta R}{\langle R\rangle}, \qquad (7)$$

where $\delta R/\langle R\rangle$ is the polydispersity of particles (the relative root-mean-square standard deviation of the nanoparticle radius from the mean value), and $\langle\lambda_0\rangle$ is the mean position of the absorption band of individual particles in the ensemble. This gives a polydispersity equal to 11%.

6. Luminescence lifetimes

Another feature of the luminescence of CQDs caused by the inhomogeneous broadening and dispersion of their properties is manifested in the measurements of their excited-state lifetimes. The luminescence decay kinetics of individual luminophores (atoms, molecules, nanoparticles) is usually monoexponential and, therefore, is characterized by one decay time. The same is true for an ensemble of identical luminophores. However, the luminescence decay kinetics for an ensemble of luminophores with different decay times is no longer monoexponential and is characterized by the distribution function of luminescence lifetimes. This is the case for CQD ensembles, where the luminescence lifetimes for individual nanoparticles vary within two-three orders of magnitude. The calculation of the distribution of decay times from the experimental decay kinetics is a complicated problem, which does not have an unambiguous solution for any nonzero noise level of the input data. In mathematics, such problems are called incorrect. They either do not have a single solution or the solution exists but is not a continuous function of the input data.

In Ref. [96], a new approach was developed for calculating the distribution of luminescence lifetimes from its experimental multiexponential decay kinetics based on the Tikhonov regularization method, taking into account the estimate of confidence intervals in the solution of linear inverse problems with the condition of nonnegative solution. This approach allows us to find solutions with almost optimal smoothness and to analyze them for the presence of artifacts related to the problem's incorrectness. The result of this approach can be demonstrated by the example of the luminescence decay kinetics for InP@ZnS CQDs [94] measured at four wavelengths (530, 550, 600, and 660 nm) shown by vertical arrows in Fig. 5. Measurements were performed at several wavelengths because the decay kinetics at different wavelengths can be different due to large inhomogeneous broadening. The kinetic curves were used to calculate the distribution of luminescence lifetimes from the expression

$$I(t) = \int_0^\infty a(\tau)\,\exp\left(-\frac{t}{\tau}\right)\mathrm{d}\ln\tau\,, \qquad (8)$$

where $I(t)$ is the luminescence decay kinetics, and $a(\tau)$ is the required probability density of the distribution of the decay time logarithm. The results of calculations are presented in Fig. 6.

The dominant broad peak in the distribution has a maximum at ≈ 35 ns. Taking into account the high quantum yield, this peak probably corresponds to the radiative lifetime

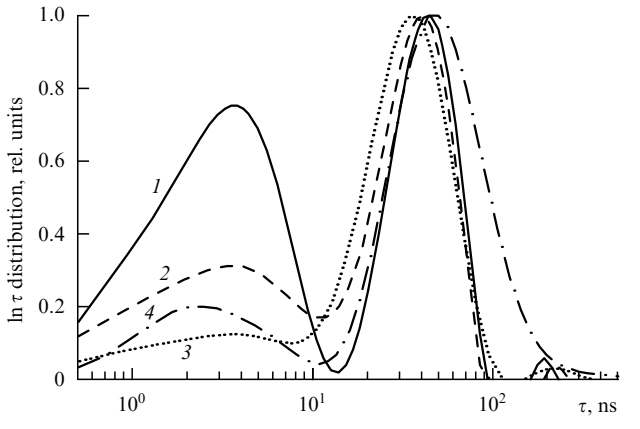

Figure 6. Distributions of the logarithm of the luminescence decay time for InP@ZnS CQDs observed at different wavelengths (see Fig. 5): 530 nm (curve *1*), 550 nm (curve *2*), 600 nm (curve *3*), and 660 nm (curve *4*). Distributions are normalized to the peak maximum for the lifetime of ≈ 35 ns. Luminescence was excited at 470 nm. The half-width of the instrumental response function was 185 ps.

of luminescence. In the short-wavelength region of the spectrum, lifetimes of about 4 ns make a great contribution. It seems that these lifetimes correspond to the strongly quenched luminescence of 'grey' CQDs. In the long-wavelength region of the spectrum, lifetimes of about 200 ns make a small but statistically reliable contribution. Because these lifetimes exceed the radiative lifetime of ≈ 35 ns, we can assume that they correspond to some trap luminescence.

It should be noted that the problem of obtaining the distribution of luminescence lifetimes from kinetic curves is incorrect in the mathematical sense. Therefore, the distributions obtained should be treated with care. They differ from true distributions at least by their considerable smoothness; the lower the signal-to-noise ratio, the higher the smoothness degree. This is manifested in Fig. 6, in particular, in that the distribution of luminescence lifetimes for kinetics measured in the long-wavelength region is so strongly smoothed that the peak at 200 ns is almost invisible.

7. Conclusion

Colloidal quantum dots can be treated as a new class of luminophores offering a number of considerable advantages over traditional luminophores. One of the most attractive advantages is the fundamental possibility of providing quite easily the required emission region in the whole visible and near-IR spectral regions by varying the emission band width from a few hundred nanometers to 20–30 nm. The fundamental possibility of obtaining very high luminescence quantum yields and high thermal stability and photostability are also important advantages. However, to realize these characteristics in practice, much effort is still required for understanding the mechanisms of photoprocesses in detail and the search for new methods for achieving the required results.

Acknowledgment
The work was supported by the Russian Scientific Foundation (project No. 14-13-01426).

References

1. Feofilov P *Usp. Fiz. Nauk* **36** 557 (1948)
2. Ekimov A I, Onushchenko A A *JETP Lett.* **34** 345 (1981); *Pis'ma Zh. Eksp. Teor. Fiz.* **34** 363 (1981)
3. Efros Al L, Efros A L *Sov. Phys. Semicond.* **16** 772 (1982); *Fiz. Tekh. Poluprovodn.* **16** 1209 (1982)
4. Brus L E *J. Chem. Phys.* **79** 5566 (1983)
5. Brus L E *J. Chem. Phys.* **80** 4403 (1984)
6. Rossetti R, Nakahara S, Brus L E *J. Chem. Phys.* **79** 1086 (1983)
7. Weller H et al. *Phys. Chem.* **88** 649 (1984)
8. Ekimov A I, Efros Al L, Onushchenko A A *Solid State Commun.* **56** 921 (1985)
9. Nozik A J et al. *J. Phys. Chem.* **89** 397 (1985)
10. Weller H, Fojtik A, Henglein A *Chem. Phys. Lett.* **117** 485 (1985)
11. Brus L *J. Phys. Chem.* **90** 2555 (1986)
12. Reed M A et al. *Phys. Rev. Lett.* **60** 535 (1988)
13. Alferov Zh I *Semicond.* **32** 1 (1998); *Fiz. Tekh. Poluprovodn.* **32** 3 (1998)
14. Chang L L, Ploog K (Eds) *Molecular Beam Epitaxy and Heterostructures* (Dordrecht: M. Nijhoff, 1985); Translated into Russian: *Molekulyarno-Luchevaya Epitaksiya i Geterostruktury* (Moscow: Mir, 1989)
15. Murray C B, Norris D J, Bawendi M G *J. Am. Chem. Soc.* **115** 8706 (1993)
16. Brichkin B S, Razumov V F *Russ. Chem. Rev.* **85** 1297 (2016); *Usp. Khim.* **85** 1297 (2016)
17. Semenoff N, Walther A *Die physikalischen Grundlagen der elektrischen Festigkeitslehre* (Berlin: Springer, 1928)
18. Fröhlich H *Physica* **6** 406 (1937)
19. Tavger B A, Demikhovskii V Ya *Sov. Phys. Usp.* **11** 644 (1969); *Usp. Fiz. Nauk* **96** 61 (1968)
20. Dingle R, Wiegmann W, Henry C H *Phys. Rev. Lett.* **33** 827 (1974)
21. Davydov A S *Quantum Mechanics* (Oxford: Pergamon Press, 1976); Translated from Russian: *Kvantovaya Mekhanika* (Moscow: GIFML, 1963)
22. Yu W W et al. *Chem. Mater.* **15** 2854 (2003)
23. Hens Z, Moreels I *J. Mater. Chem.* **22** 10406 (2012)
24. Rajh T, Mićić O I, Nozik A J *J. Phys. Chem.* **97** 11999 (1993)
25. Leatherdale C A et al. *J. Phys. Chem. B* **106** 7619 (2002)
26. de Mello Donegá C, Koole R *J. Phys. Chem. C* **113** 6511 (2009)
27. Vossmeyer T et al. *J. Phys. Chem.* **98** 7665 (1994)
28. Milekhin A G et al. *Phys. Solid State* **44** 1976 (2002); *Fiz. Tverd. Tela* **44** 1884 (2002)
29. Biswas S et al. *Chin. J. Phys.* **49** 92 (2011)
30. Kumar P et al. *Physica B* **407** 3347 (2012)
31. Singha A et al. *J. Phys. Condens. Matter* **17** 5697 (2005)
32. Dzhagan V et al. *Int. J. Spectrosc.* **532** 385 (2012)
33. Nirmal M et al. *Nature* **383** 802 (1996)
34. Fernee M J, Tamarat P, Lounis B *Chem. Soc. Rev.* **43** 1311 (2014)
35. Schmidt R et al. *ACS Nano* **8** 3506 (2014)
36. Cui J et al. *Chem. Soc. Rev.* **43** 1287 (2014)
37. Ko H-C, Yuan C-T, Tang J *Nano Rev.* **2** 5895 (2011)
38. Schwartz O, Oron D *Isr. J. Chem.* **52** 992 (2012)
39. Shibu E S et al. *Coord. Chem. Rev.* **263** 2 (2014)
40. Efros Al L, Rosen M *Phys. Rev. Lett.* **78** 1110 (1997)
41. Osad'ko I S *Fluktuiruyushchaya Fluorestsentsiya Nanochastits* (Blinking Fluorescence of Nanoparticles) (Moscow: Fizmatlit, 2011)
42. Califano M *J. Phys. Chem. C* **115** 18051 (2011)
43. Cordones A A, Bixby T J, Leone S R *J. Phys. Chem. C* **115** 6341 (2011)
44. Durisic N et al. *ACS Nano* **3** 1167 (2009)
45. Galland C et al. *Nature* **479** 203 (2011)
46. Frantsuzov P A, Volkán-Kacsó S, Jankó B *Phys. Rev. Lett.* **103** 207402 (2009)
47. Zhao J et al. *Phys. Rev. Lett.* **104** 157403 (2010)
48. Osad'ko I S *Phys. Usp.* **59** 462 (2016); *Usp. Fiz. Nauk* **186** 489 (2016)
49. Ebenstein Y, Mokari T, Banin U *Appl. Phys. Lett.* **80** 4033 (2002)
50. Brokmann X et al. *Phys. Rev. Lett.* **93** 107403 (2004)
51. Tenne R et al. *ACS Nano* **7** 5084 (2013)
52. Chen Y et al. *J. Am. Chem. Soc.* **130** 5026 (2008)
53. Dennis A M et al. *Nano Lett.* **12** 5545 (2012)
54. Mahler B et al. *Nature Mater.* **7** 659 (2008)
55. Chen O et al. *Nature Mater.* **12** 445 (2013)
56. Veilleux V et al. *Nanotechnology* **21** 134024 (2010)
57. Chon B et al. *Phys. Chem. Chem. Phys.* **12** 9312 (2010)
58. Dong C et al. *Chem. Eur. J.* **20** 1940 (2014)
59. Zan F et al. *J. Phys. Chem. C* **116** 3944 (2012)
60. Hohng S, Ha T *J. Am. Chem. Soc.* **126** 1324 (2004)
61. Durisic N et al. *ACS Nano* **5** 9062 (2011)
62. Fu Y, Zhang J, Lakowicz J R *Chem. Phys. Lett.* **447** 96 (2007)
63. Jin S, Song N, Lian T *ACS Nano* **4** 1545 (2010)
64. Yuan C T et al. *ACS Nano* **3** 3051 (2009)
65. Hamada M et al. *ACS Nano* **4** 4445 (2010)
66. Schaller R D et al. *Nano Lett.* **6** 424 (2006)
67. Schaller R D, Klimov V I *Phys. Rev. Lett.* **92** 186601 (2004)
68. Nair G et al. *Phys. Rev. B* **78** 125325 (2008)
69. Midgett A G et al. *Nano Lett.* **13** 3078 (2013)
70. Califano M *ACS Nano* **5** 3614 (2011)
71. Kobayashi Y, Udagawa T, Tamai N *Chem. Lett.* **38** 830 (2009)
72. Pijpers J J H et al. *J. Phys. Chem. C* **111** 4146 (2007)
73. Stubbs S K et al. *Phys. Rev. B* **81** 081303(R) (2010)
74. Trinh M T et al. *Nature Photon.* **6** 316 (2012)
75. Nozik A J *Annu. Rev. Phys. Chem.* **52** 193 (2001)
76. Cho B et al. *Nano Lett.* **10** 2498 (2010)
77. Smith C, Binks D *Nanomaterials* **4** 19 (2014)
78. Schaller R D, Agranovich V M, Klimov V I *Nature Phys.* **1** 189 (2005)
79. Shabaev A, Efros Al L, Nozik A J *Nano Lett.* **6** 2856 (2006)

80. Sambur J B, Novet T, Parkinson B A *Science* **330** 63 (2010)
81. Semonin O E et al. *Science* **334** 1530 (2011)
82. Beard M C et al. *Nano Lett*. **9** 836 (2009)
83. Yang Y, Rodríguez-Córdoba W, Lian T *Nano Lett*. **12** 4235 (2012)
84. Tovstun S A, Razumov V F *High Energy Chem*. **49** 352 (2015); *Khim. Vysok. Energ*. **49** 394 (2015)
85. Kennard E H *Phys. Rev*. **11** 29 (1918)
86. Mazurenko Yu T, Neporent B S *Opt. Spectrosc*. **12** 317 (1962); *Opt. Spektrosk*. **12** 571 (1962)
87. Stepanov B I *Sov. Phys. Dokl*. **2** 81 (1957); *Dokl. Akad. Nauk SSSR* **112** 839 (1957)
88. van Roosbroeck W, Shockley W *Phys. Rev*. **94** 1558 (1954)
89. Ketskeméty I, Dombi J, Horvai R *Acta Phys. Acad. Sci. Hung*. **12** 263 (1960)
90. Levshin V L *J. Appl. Spectrosc*. **7** 319 (1967); *Zh. Prikl. Spektrosk*. **7** 466 (1967)
91. Temkin H et al *J. Appl. Phys*. **52** 1574 (1981)
92. Muth J F et al. *Appl. Phys. Lett*. **71** 2572 (1997)
93. Ullrich B, Munshi S R, Brown G J *Semicond. Sci. Technol*. **22** 1174 (2007)
94. Brichkin S B *High Energy Chem*. **50** 395 (2016); *Khim. Vysok. Energ*. **50** 417 (2016)
95. Mičič O I, Ahrenkiel S P, Nozik A J *Appl. Phys. Lett*. **78** 4022 (2001)
96. Tovstun S A *High Energy Chem*. **50** 327 (2016); *Khim. Vysok. Energ*. **50** 345 (2016)